

1  
2  
3  
4 **In Vivo Intravascular Ultrasound Imaging of Fibromuscular Dysplastic**  
5  
6  
7 **Region and Intravascular Pressure Gradient-Guided Percutaneous**  
8  
9  
10 **Transluminal Renal Angioplasty**  
11  
12  
13  
14

15 Onoue et al      Running title: IVUS- and Pressure Gradient-Guided Renal Angioplasty  
16  
17  
18  
19  
20  
21  
22

23 Yoshiro Onoue, MD; Kenichi Tsujita, MD, PhD; Seiji Hokimoto, MD, PhD; Koichi Kaikita, MD,  
24  
25                      PhD; Seigo Sugiyama, MD, PhD; Hisao Ogawa, MD, PhD, FJCC  
26  
27  
28  
29

30 From the Department of Cardiovascular Medicine, Faculty of Life Sciences, Graduate School of  
31  
32 Medical Sciences, Kumamoto University, Kumamoto, Japan (Y.O., K.T., S.H., K.K., S.S., H.O.).  
33  
34  
35  
36  
37  
38  
39

40 Correspondence to: Kenichi Tsujita, MD, PhD,  
41

42 1-1-1 Honjo, Kumamoto 860-8556, Japan.  
43

44 Phone: +81-96-373-5175, Fax: +81-96-362-3256, E-mail: tsujita@kumamoto-u.ac.jp  
45  
46  
47  
48  
49

50 **Key Words:** intravascular ultrasound; renal artery stenosis; renal pressure gradients;  
51  
52 renovascular hypertension; vascular interventions  
53  
54  
55  
56

57 Total Word Count: 1613  
58  
59  
60  
61  
62  
63  
64  
65

1  
2  
3  
4 **Abstract**  
5

6  
7 Fibromuscular dysplasia (FMD) is one of the etiologies of renal artery stenosis (RAS) and  
8  
9 secondary hypertension. Balloon angioplasty has emerged as the mainstay of treatment because  
10  
11 patients with FMD usually show substantial clinical and anatomic response to renal angioplasty  
12  
13 without stenting. We report a 21-year-old male case of FMD-induced RAS treated with  
14  
15 intravascular ultrasound- and pressure gradient-guided renal angioplasty. Ultrasonic imaging of  
16  
17 the stenotic renal artery clearly visualized adventitial fibrotic band surrounding the negative  
18  
19 remodeled renal artery and the accompanied atherosclerotic plaque. The findings suggest that  
20  
21 atherosclerotic change can occur in young patients with renal FMD that is basically considered to  
22  
23 be *non*atherosclerotic. Pressure gradient measurement is also useful in confirming hemodynamic  
24  
25 improvement during angioplasty.  
26  
27  
28  
29  
30  
31  
32  
33  
34  
35  
36  
37  
38  
39  
40  
41  
42  
43  
44  
45  
46  
47  
48  
49  
50  
51  
52  
53  
54  
55  
56  
57  
58  
59  
60  
61  
62  
63  
64  
65

1  
2  
3  
4 **Introduction**  
5

6  
7 Fibromuscular dysplasia (FMD) is one of the causes of renal artery stenosis (RAS), and is  
8  
9 generally considered a nonatherosclerotic vascular disease. Although FMD RAS is characterized  
10  
11 by angiographic “string of beads” appearance, the typical angiographic morphology is absent in  
12  
13 some cases. Also, the optimal endpoint of interventional revascularization for RAS has not been  
14  
15 clearly established. Here, we present an interesting case of FMD RAS evaluated by  
16  
17 multimodality such as intravascular ultrasound (IVUS), scintigraphy, and intravascular pressure  
18  
19 gradient.  
20  
21  
22

23 **Case Report**  
24

25  
26 A 21-year-old man with drug-resistant hypertension was admitted to our institute. Both baseline-  
27  
28 and captopril-renoscintigraphy revealed the decrease on the left kidney’s glomerular filtration  
29  
30 rate (GFR) and captopril-induced additional GFR reduction (Figure 1). A computed tomography,  
31  
32 magnetic resonance angiography and renal arteriography (Figures 2 and 3) demonstrated the left  
33  
34 RAS that seemed to be accountable for activated renin-aldosterone system (plasma renin activity  
35  
36 [PRA, 5.6 ng/ml/hr] and plasma aldosterone concentration [PAC, 233 pg/ml]); thus, he was  
37  
38 scheduled to undergo percutaneous transluminal renal angioplasty (PTRA). The distal renal  
39  
40 artery and aortic pressures were recorded with a pressure gradient of 70 mmHg (Figure 4). IVUS  
41  
42 identified decreased lumen areas and concentric fibrotic band surrounding the stenosis (Figure 3).  
43  
44 Also, IVUS visualized that distal part of the stenosis was accompanied with eccentric  
45  
46 atherosclerotic plaque. IVUS-derived iMap™ tissue characterization software (Boston Scientific  
47  
48 Corp., Natick, MA) recognized the segmental adventitial layer as “fibrotic” hyperplasia. The  
49  
50 fibrotic lesion could be easily dilated by 3.0- and 3.5-mm balloons with nominal dilatation  
51  
52 pressure. Post-PTRA IVUS revealed an increased lumen area and vessel expansion without any  
53  
54  
55  
56  
57  
58  
59  
60  
61  
62  
63  
64  
65

1  
2  
3  
4 dissection. The peak-to-peak systolic pressure gradient across the stenosis decreased from 70  
5  
6 mmHg to 10 mmHg. Post-PTRA renoscintigraphy showed the improvement on the GFR, and his  
7  
8 activated renin-aldosterone system was promptly normalized (PRA, 0.3 ng/ml/hr; PAC, 18.2  
9  
10 pg/ml).  
11  
12

### 13 14 **Discussion**

15  
16 FMD is generally considered a nonatherosclerotic vascular disease that affects the renal and  
17  
18 internal carotid arteries commonly. Renal FMD occurs in the middle or distal arterial segments in  
19  
20 younger patients with few cardiovascular risk factors, while atherosclerotic RAS typically occurs  
21  
22 at the ostium and proximal portions in older patients with multiple risks. In the current case,  
23  
24 FMD was easily presumed as a primary cause of RAS from the anatomical and clinical features,  
25  
26 however, typical "string of beads" appearance was not observed on the angiogram. Unlike  
27  
28 common medial FMD, adventitial FMD was reported to be very rare and may have a focal  
29  
30 stenotic appearance.<sup>1</sup> IVUS imaging of the stenotic renal artery clearly visualized adventitial  
31  
32 fibrotic band surrounding the negative remodeled renal artery and the accompanied  
33  
34 atherosclerotic plaque, suggesting that atherosclerotic change can occur in young patients with  
35  
36 renal FMD that has been basically considered to be *non*atherosclerotic. Consistent with  
37  
38 pathologic study which showed that the fibroplastic lesion was characterized by a dense  
39  
40 accumulations of elastic tissue,<sup>2</sup> the dysplastic region was homogeneously fibrotic in grayscale  
41  
42 IVUS, and was coded as uniformly fibrotic tissue in iMap™ software as well.  
43  
44  
45  
46  
47  
48  
49

50  
51 The use of stents for FMD has been reserved as a "bailout" procedure in cases in which  
52  
53 there are suboptimal results with balloon angioplasty or in which renal artery dissection occurs,  
54  
55 because patients with FMD usually show substantial clinical and anatomic response to PTRA  
56  
57 without stenting.<sup>3</sup> Especially in the current young case, renal stenting, that necessitates indefinite  
58  
59  
60  
61  
62  
63  
64  
65

1  
2  
3  
4 aspirin intake, should be avoided to the extent possible. In atherosclerotic RAS, a systolic  
5  
6 pressure gradient of >20 mmHg may more accurately detect a clinically significant stenosis.<sup>4</sup> In  
7  
8 the current case, the pressure gradient reduction from 70 mmHg to 10 mmHg was associated  
9  
10 with the improvement of renal blood flow and normalization of renin-aldosterone system.  
11

12  
13  
14 Taken together, the combination use of IVUS and intravascular pressure gradient  
15  
16 provides us decision-making safety (absence of post-PTRA renal artery perforation/dissection by  
17  
18 IVUS) and efficacy (post-PTRA lumen enlargement by IVUS and hemodynamic improvement  
19  
20 by intravascular pressure gradient) information during PTRA.  
21

### 22 23 24 **Conclusion**

25  
26 In conclusion, such multimodality work-up could be useful for etiological evaluation in patients  
27  
28 with RAS, and might lead to optimal strategy in PTRA for RAS.  
29  
30

### 31 32 33 **Disclosures**

34  
35  
36 None.  
37  
38  
39

### 40 41 42 **Acknowledgment**

43  
44 This work was supported in part by grants-in-aid for scientific research from the Ministry of  
45  
46 Education, Culture, Sports, Science and Technology, Japan.  
47  
48  
49

### 50 51 52 **References**

- 53 **1.** Slovit DP, Olin JW. Fibromuscular dysplasia. *N Engl J Med.* 2004;350:1862-71.  
54
- 55 **2.** Stanley JC, Gewertz BL, Bove EL, Sottiurai V, Fry WJ. Arterial fibrodysplasia.  
56  
57 Histopathologic character and current etiologic concepts. *Arch Surg.* 1975;110:561-6.  
58  
59  
60  
61

1  
2  
3  
4  
5  
6  
7  
8  
9  
10  
11  
12  
13  
14  
15  
16  
17  
18  
19  
20  
21  
22  
23  
24  
25  
26  
27  
28  
29  
30  
31  
32  
33  
34  
35  
36  
37  
38  
39  
40  
41  
42  
43  
44  
45  
46  
47  
48  
49  
50  
51  
52  
53  
54  
55  
56  
57  
58  
59  
60  
61  
62  
63  
64  
65

3. Rundback JH, Sacks D, Kent KC, Cooper C, Jones D, Murphy T, Rosenfield K, White C, Bettmann M, Cortell S, Puschett J, Clair D, Cole P. Guidelines for the reporting of renal artery revascularization in clinical trials. American Heart Association. *Circulation*. 2002;106:1572-85.
4. Gross CM, Kramer J, Weingartner O, Uhlich F, Luft FC, Waigand J, Dietz R. Determination of renal arterial stenosis severity: comparison of pressure gradient and vessel diameter. *Radiology*. 2001;220:751-6.

1  
2  
3  
4 **Legends to Figures**  
5

6  
7 **Figure 1.** Baseline- and captopril-renoscintigraphy with Tc-99m diethylene triamine penta-acetic  
8 acid (DTPA). (A) Before percutaneous transluminal renal angioplasty (PTRA),  
9 baseline-99mTc-DTPA renoscintigraphy demonstrated the decrease on the left kidney's  
10 glomerular filtration rate (GFR, 22.2 ml/min). Captopril-99mTc-DTPA renoscintigraphy showed  
11 that GFR of the left kidney was lowered than that of the control (captopril-induced reduction rate  
12 [CRR, 17.4%], which was calculated from the renal uptake before [22.2 ml/min] and after [18.4  
13 ml/min] captopril), while GFR of the right kidney increased by captopril loading. (B) Post-PTRA  
14 renoscintigraphy showed the improvement on the left kidney's GFR and CRR (2.2% from 17.4%  
15 at pre-PTRA)  
16  
17  
18  
19  
20  
21  
22  
23  
24  
25  
26  
27  
28  
29  
30

31 **Figure 2.** Noninvasive morphological evaluation of renal artery stenosis. (A) A computed  
32 tomography angiography visualized tandem lesion at middle segment of the left renal artery.  
33 Note the location of stenosis and absence of atherosclerotic change such as arterial wall  
34 irregularity and calcification. (B) A magnetic resonance angiography demonstrated the severe  
35 stenosis at middle to distal segment of left renal artery as well. (C) The left kidney was mildly  
36 atrophic compared with right kidney.  
37  
38  
39  
40  
41  
42  
43  
44  
45  
46  
47

48 **Figure 3.** The pre- and post-PTRA selective left renal arteriogram (top and bottom) and serial  
49 grayscale IVUS and IVUS-derived tissue component of fibromuscular dysplastic region.  
50 Consistent with computed tomography and magnetic resonance angiography, pre-percutaneous  
51 transluminal renal angioplasty (PTRA) selective left renal arteriogram (on the top) showed  
52 tandem lesion at middle segment of left renal artery. (A) At proximal portion of the stenotic  
53  
54  
55  
56  
57  
58  
59  
60  
61  
62  
63  
64  
65

1  
2  
3  
4 lesion, grayscale intravascular ultrasound (IVUS) visualized severely negative remodeled renal  
5  
6 artery and thick fibrotic band surrounding the stenosis. The region was fibrotic and appeared to  
7  
8 involve the adventitia. Note the absence of atherosclerotic plaque at the segment. **(A')** The  
9  
10 cross-sectional IVUS panel corresponds to pre-PTRA cross-sectional IVUS image "A." The  
11  
12 negative remodeled renal artery was dramatically expanded by balloon angioplasty without any  
13  
14 renal artery dissection. Note the small renal vein at 9-10 o'clock on the pre- and post-PTRA  
15  
16 IVUS images that corresponds to the same small renal vein on the IVUS images. **(B)** At distal  
17  
18 portion of the stenotic lesion, grayscale IVUS identified decreased lumen areas and concentric  
19  
20 fibrotic band surrounding the stenosis as well as the proximal portion. Unlike the proximal  
21  
22 segment, here eccentric atherosclerotic plaque was accompanied with fibromuscular dysplasia at  
23  
24 1-6 o'clock. Newly developed IVUS-based tissue characterization software (iMap™)  
25  
26 demonstrates the ability to characterize coronary plaque tissue using an IVUS + radiofrequency  
27  
28 system. Using 40MHz mechanical IVUS transducer, iMap™ analysis coded tissue as light-green  
29  
30 (fibrotic), yellow (lipidic), pink (necrotic), and light-blue (calcified). The iMap™ tissue  
31  
32 characterization software recognized both the atherosclerotic plaque (left panel of (B)) and the  
33  
34 segmental adventitial layer (right panel of (B)) as "fibrotic." It is also worth noting that the  
35  
36 FMD-associated atherosclerotic plaque was not highly atherosclerotic, such as calcified and  
37  
38 necrotic plaque. **(B')** The cross-sectional IVUS panel corresponds to pre-PTRA cross-sectional  
39  
40 IVUS image "B." The fibromuscular dysplastic region was successfully dilated by balloon  
41  
42 angioplasty without any dissection. Note the small renal vein at 10-11 o'clock on the pre- and  
43  
44 post-PTRA IVUS images that corresponds to the same small renal vein on the IVUS images.  
45  
46  
47  
48  
49  
50  
51  
52  
53  
54  
55  
56  
57

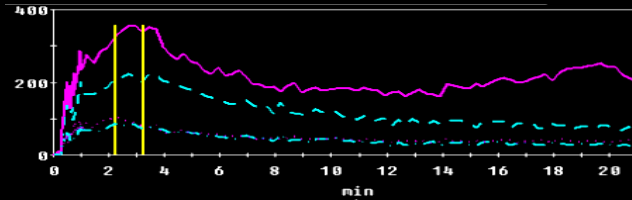
58 **Figure 4.** Pre- and post-PTRA PressureWire measurement depicting the phasic and mean  
59  
60  
61  
62  
63  
64  
65



1  
2  
3  
4 proximal renal artery pressure, phasic and mean distal renal artery pressure, and the mean distal  
5  
6 to proximal artery pressure ratio. **(A)** Using a PressureWire™ Certus (St. Jude Medical, St. Paul,  
7  
8 MN), the distal renal artery and aortic pressures were recorded with a pressure gradient of 70  
9  
10 mmHg. **(B)** After successful percutaneous transluminal renal angioplasty, the distal renal artery  
11  
12 to proximal renal artery peak-to-peak systolic gradient across the stenosis decreased to  
13  
14 approximately 10 mmHg.  
15  
16  
17  
18  
19  
20  
21  
22  
23  
24  
25  
26  
27  
28  
29  
30  
31  
32  
33  
34  
35  
36  
37  
38  
39  
40  
41  
42  
43  
44  
45  
46  
47  
48  
49  
50  
51  
52  
53  
54  
55  
56  
57  
58  
59  
60  
61  
62  
63  
64  
65

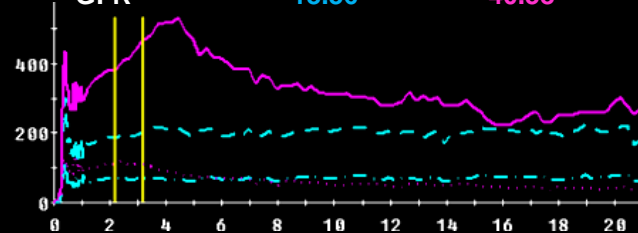


Kidney      Left      Right  
 GFR          22.23      36.34



**Captopril (-)**

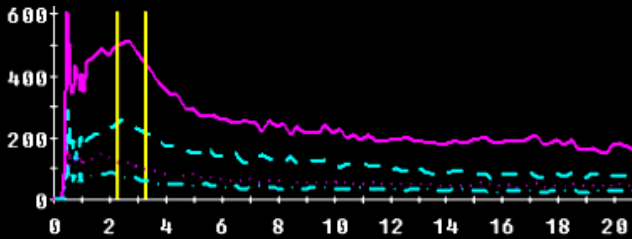
Kidney      Left      Right  
 GFR          18.36      40.38



**Captopril (+)**

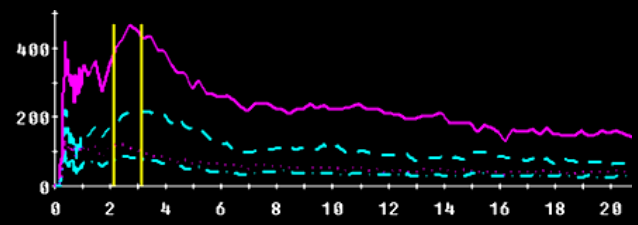
# A. Pre-PTRA

Kidney      Left      Right  
 GFR          17.8      36.72



**Captopril (-)**

Kidney      Left      Right  
 GFR          17.43      37.24



**Captopril (+)**

# B. Post-PTRA

**Figure 1**

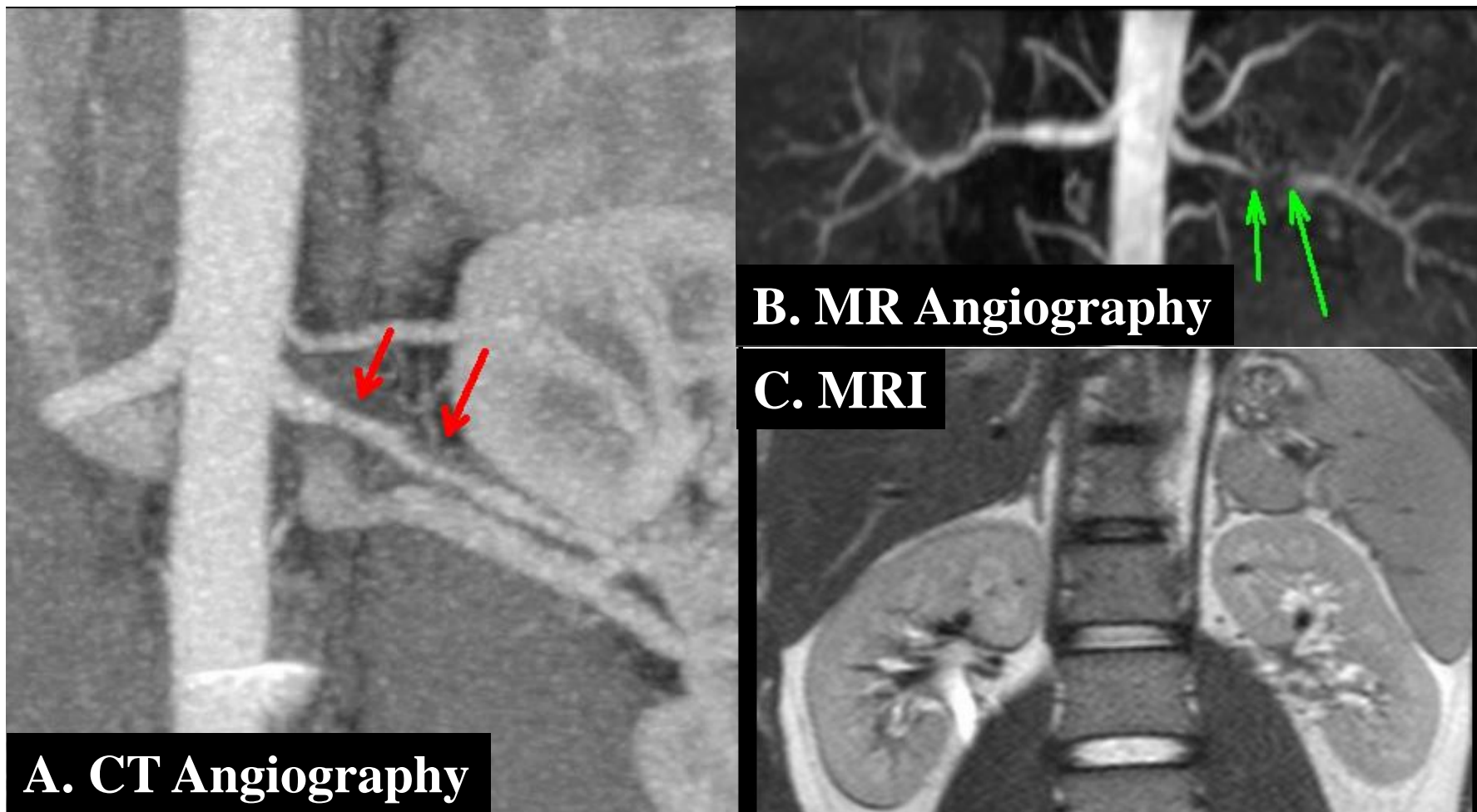
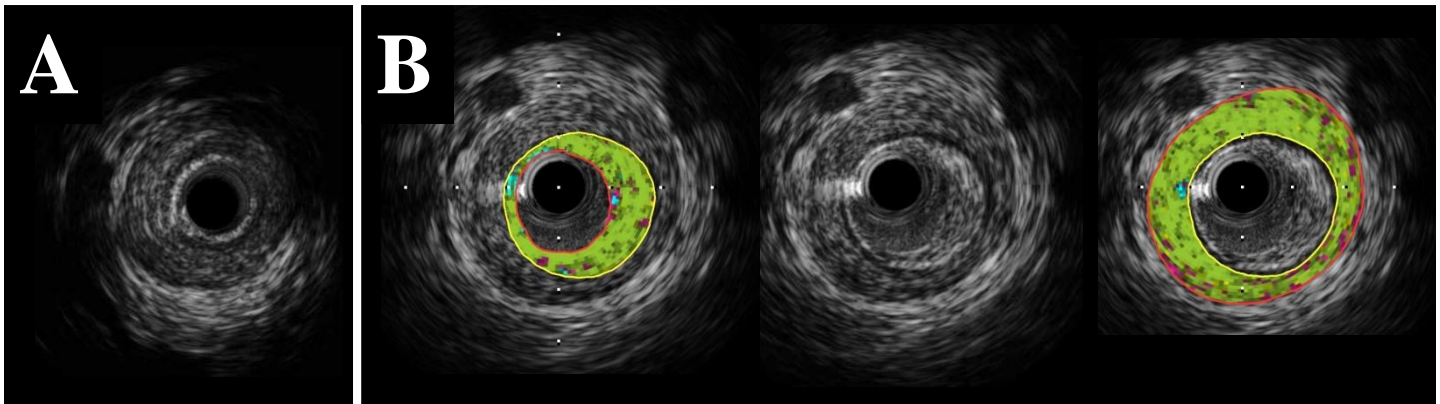


**Figure 2**

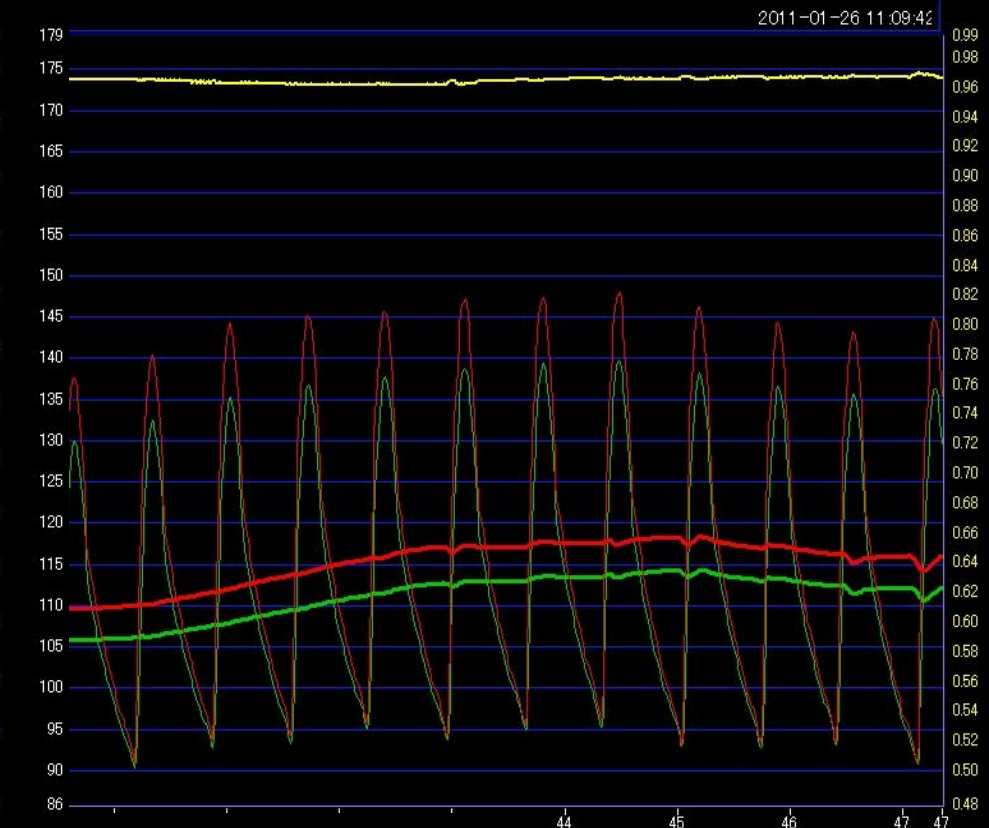
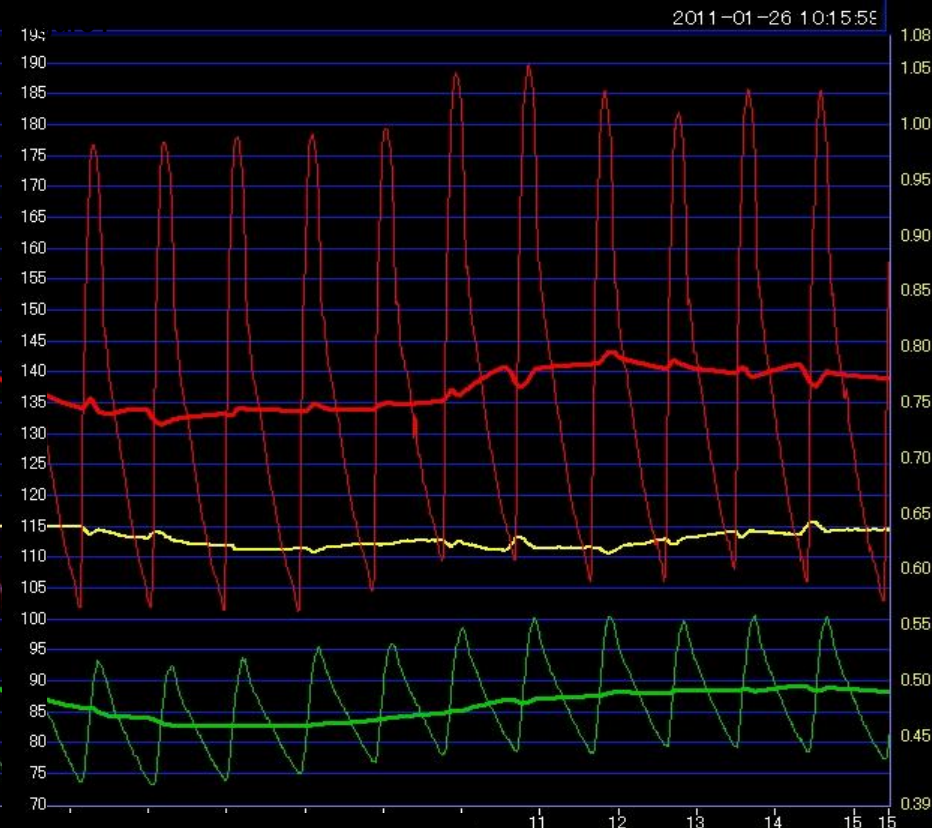
**Pre-PTRA**



**Post-PTRA**

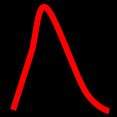




**Figure 3**



**A. Pre-PTRA**

**B. Post-PTRA**

 **Phasic Proximal Renal Artery Pressure**  
 **Mean Proximal Renal Artery Pressure**  
 **Mean Distal to Proximal Artery Pressure Ratio**

 **Phasic Distal Renal Artery Pressure**  
 **Mean Distal Renal Artery Pressure**

**Figure 4**